



Features and impacts of currents and waves on sediment resuspension in a large shallow lake in China

Wenhao Ding^{1,2} · Tingfeng Wu¹ · Boqiang Qin¹ · Yingtien Lin³ · Han Wang⁴

Received: 13 July 2018 / Accepted: 16 October 2018 / Published online: 27 October 2018
© Springer-Verlag GmbH Germany, part of Springer Nature 2018

Abstract

Wind-induced hydrodynamics are important forcing mechanisms of sediment resuspension in lakes. However, the relative contributions of wind-induced waves and currents on sediment resuspension during a wind event remain unclear. This study used high-frequency sensors to investigate the effects of wind waves, lake currents, and shear stress on sediment resuspension under different wind conditions (10 September to 17 October 2017) in Lake Taihu (China). Measurements showed that wind speed varied from 0.3 to 11.5 m/s, wave height varied from 0.035 to 0.46 m, lake current speed ranged from 0.001 to 0.39 m/s, and turbidity changed from 36.5 to 158.7 NTU. Sediment resuspension resulted primarily from wave- and current-induced shear stresses. Calculation showed these quantities varied in the range 0.045–0.338 and 0.002–0.127 N/m², respectively. Total shear stress showed positive correlation with turbidity. Wave-induced shear stress contributed more than 60% of the total. Waves and currents have different responses to wind. During periods of increasing turbidity, the percentage of wave-induced shear stress was initially high (> 85%) before decreasing with the development of the current. During periods of decreasing turbidity, the percentage of wave-derived shear stress declined initially before increasing with the decrease of current speed. The results showed a clear process regarding the contributions of shear stress from waves and currents during different stages of hydrodynamic development, which could be used to describe sediment resuspension in large shallow lakes that would help in the development of high-efficiency sediment resuspension models.

Keywords Wind · Waves · Currents · Sediment resuspension · Shallow lake

Introduction

Currents and waves represent fundamental physical processes that have important effects on the ecosystems of the large shallow lakes (Qin 2008; Chen et al. 2013; Yan et al. 2017). Sediment resuspension is one of the consequences of such

hydrodynamic processes (Bailey and Hamilton 1997; Koch 1999; Jin and Sun 2007; Stastna and Lamb 2008; Huang et al. 2015). It can be triggered by wind-wave- and current-induced shear stresses (Qin 2008), and release to the water column pollutants that constitute one of the main sources of eutrophication (Søndergaard et al. 1992; Olsson et al. 1997;

Responsible editor: Philippe Garrigues

✉ Tingfeng Wu
tfwu@niglas.ac.cn

✉ Boqiang Qin
qinbq@niglas.ac.cn

Wenhao Ding
whding@niglas.ac.cn

Yingtien Lin
kevinlin@zju.edu.cn

Han Wang
wanghst@hhu.edu.cn

¹ State Key Laboratory of Lake Science and Environment, Nanjing Institute of Geography and Limnology, Chinese Academy of Sciences, 73 East Beijing Road, Nanjing 210008, People's Republic of China

² University of Chinese Academy of Sciences, Beijing 100049, China

³ Ocean College, Zhejiang University, 1 Zheda Road, Zhoushan 316000, People's Republic of China

⁴ State Key Laboratory of Hydrology-Water Resources and Hydraulic Engineering, Hohai University, 1 Xikang Road, Nanjing 210098, People's Republic of China

Qin et al. 2004; Tan 2012; Zhu et al. 2017). Sediment resuspension occurs frequently in shallow lakes because calm conditions seldom occur, and because the substantial current and wave effects induced by wind can cause disturbances that are able to reach the bottom of the water column (Wu et al. 2013; Zhao et al. 2018).

The features of currents and waves in large shallow lakes are markedly different from other water bodies (Qin et al. 2007; Preusse et al. 2010). Generally, a thermocline does not exist because of both the shallow depth (Li et al. 2011) and the heterogeneity of the covering wind field related to the large scale (Ozger 2010; Vanem and Walker 2013). These features of lakes determine the specific hydrodynamic attributes. Many studies that have addressed sediment resuspension in lakes have focused on environmental effects such as nutrient release (Lawson et al. 2012; Wang et al. 2015) and light availability (Lawson 2004; Wiberg 2007). Clear understanding of the mechanisms of sediment resuspension will provide a basis for the development of appropriate models that could facilitate efficient and healthy management of lakes.

Lake Taihu (China) is a severely eutrophic large shallow lake with considerable deposits of sediment (Qin et al. 2006; Hu et al. 2006). Wind, inflow–outflow, frequent anthropogenic activities, and bottom terrain all affect the physical processes of the water. The influences from these factors together with the special shape of the lake determine the complex structures of the currents and waves (Luettich and Somlyódy 1990; Qin 2008; Wu et al. 2013). The shear stresses produced by currents and waves constitute the primary factors governing sediment resuspension (Amos and Mosher 1985; James et al. 1997; Chung et al. 2009). The relationship between critical shear stress and sediment erosion has been studied in relation to Lake Okeechobee (FL, USA) (Mehta et al. 2015). Furthermore, a study on the impacts of wind waves on sediment transport has also been undertaken in the same lake (Ji and Jin 2014). The relationship between turbidity and wave action has been studied in Lake Erie (North America) (Paul et al. 1982), and sediment resuspension has been recognized as one of the most important factors with regard to eutrophication (Tan 2012). However, the mechanisms of sediment resuspension under the influence of hydrodynamics remain unclear, and this lack of knowledge hinders effective research on the ecological effects of sediment resuspension. Furthermore, the development of hydrodynamic models is closely linked with the parameters that produce wave- and current-induced effects on sediment. Therefore, quantification of the contributions of the shear stresses derived from waves and currents will help elucidate the mechanisms of sediment resuspension, as well as accelerate the development of hydrodynamic models.

To investigate the characteristics of wind-induced waves and currents, as well as their contributions to sediment resuspension, in situ long-term synchronous field observations of winds and wind-induced waves, currents, and turbidity were undertaken in Lake Taihu. The objectives of the study were twofold: (1) to identify the characteristics of wind-induced waves and currents, and to explore the relationships between wind conditions and wind-induced waves; and (2) to quantify the relative contributions of the shear stresses of waves and currents to sediment resuspension.

Methods and materials

Study site

Lake Taihu, located in the Yangtze River Delta (30.93–31.55° N, 119.88–120.60° E), is the third largest freshwater lake in China. The lake has a surface area of 2338.1 km², with mean water depths of 1.9 m. The water quality of Lake Taihu has been deteriorating since the 1950s (Qin et al. 2006) in conjunction with an increase in external nutrient loading. Over-enrichment by nitrogen and phosphorus can promote algal blooms (Ma et al. 2014), and Lake Taihu has experienced severe algal blooms, which have caused drinking water crises in the city of Wuxi (Qin et al. 2010). Previous research has identified that considerable amounts of nitrogen and phosphorus released from sediment can influence the development of algal blooms (Qin et al. 2006; Møller and Riisgård 2007; Ma et al. 2016). The release of nitrogen and phosphorus from sediment has a close relationship with lake hydrodynamics and bottom stress is fundamental to sediment resuspension. When bottom stress is larger than the crucial shear stress required for the resuspension of sediment, resuspension will occur (Wilcock 1993; Qin 2008). In Lake Taihu, there is no significant variation in sediment particle size (10–15 μm) with either depth or region; therefore, the critical shear stress in Lake Taihu is determined mainly by sediment density (Qin et al. 2004).

Data collection

The arrangement of the stations for data collection was designed to satisfy the requirements of observing different parameters to study the influences of waves and currents on the sediment (Fig. 1). In Lake Taihu, change in the wind direction can have considerable influence on fetch. Therefore, the station (no. 2) at which the currents and waves were observed in this study was located in the center of the lake, such that the distance to the lake bank (and thus the fetch) was similar in all directions. Consequently, we consider that wind direction had limited influence on our results. At site no.1, no.2, and no. 3 in the central part of the lake, three 5-m-high platforms were

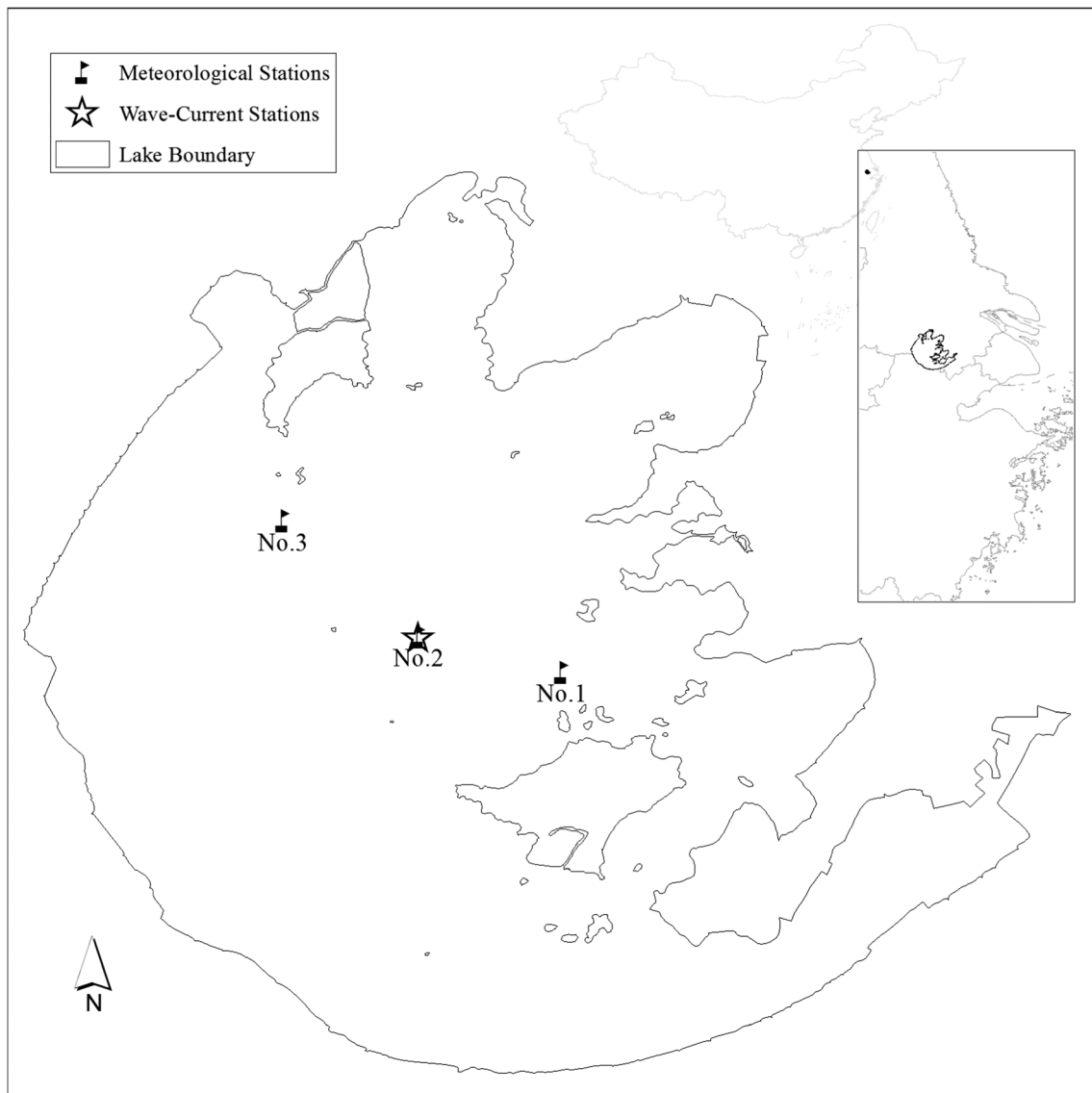


Fig. 1 Location and plan of Lake Taihu (China) showing the positions of the three meteorological stations and the location of the wave–current–turbidity monitors

built to facilitate the acquisition of the detailed measurements. The water depth at these stations ranged from 2.8 to 3.2 m during the observation period.

Meteorological instrumentation

To investigate the influence of the wind forcing on the wave and current fields, meteorological stations were deployed on platforms constructed at site no. 1 (31.21° N, 120.27° E; eastern part of Lake Taihu, north of the Xishan Islands with several small islands nearby), site no. 2 (31.23° N, 120.17° E; central part of Lake Taihu with surrounding open water), and site no. 3 (31.31° N, 120.07° E; connection between Meiliang Bay and Zhushan Bay). The distribution of these three stations was aligned with the predominant wind direction. Meteorological variables were measured at

each of these sites using a portable weather station (WXT520; Vaisala Inc., Finland) with 1-min intervals and the 5-min mean values of wind speed and wind direction were recorded. The stations were in operation from 9 September 2017 to 17 October 2017. After collection, the wind data were converted to standard wind data, 10 m above the water surface (CERC 1984).

Wind waves

Surface waves were measured using an 8-Hz MIDAS wave recorder (Valeport Ltd., U.K.) with a pressure sensor. The instrument recorded both wave and tidal components. Overall, 1024 wave samples were measured and 30-min mean values were recorded. The equipment was mounted within a steel frame on the bottom of the lake to ensure the sensor

remained immobile. This wave sensor was located at station no. 2.

Wind-driven currents

An acoustic Doppler current profiler (ADCP, SonTek, USA) was used to observe the lake currents. The currents were measured with a frequency of 2 Hz, and the derived currents were output every 15 min. The ADCP was mounted with an upward-looking orientation on a steel plate, and the ultrasonic beam was sent from the bottom to the water surface. The layer thickness for the acoustic wave was set as 0.4 m during the investigation. The monitor recorded the velocity of the current every 0.4 m from 0.7 m (height of the equipment and thickness of the dead zone) above the bottom to the set height of 4.0 m. This current sensor was located at station no. 2.

Observation of turbidity

Water turbidity was measured using an YSI 6600V2-2 (USA) equipped with a self-cleaning turbidity probe. The equipment was positioned near the bottom of the lake, 0.8 m above the bed and about 2.0 m below the water surface. It recorded turbidity at 60-min intervals from 9 September 2017 to 17 October 2017. This turbidity sensor was located at station no. 2.

Analysis methods

Wind-induced hydrodynamics, including waves and currents, have considerable impact on sediment resuspension. Generally, wind-wave- and current-induced shear stresses are considered when calculating sediment resuspension.

Wind data processing method

In accordance with a previous study, the acquired wind speeds were transformed to the reference height of 10 m above the water surface, using the following logarithmic profile law:

$$U_{10} = U_{\text{measured}} \left(\frac{\ln\left(\frac{10}{z_0}\right)}{\ln\left(\frac{z}{z_0}\right)} \right), \quad (1)$$

where U_{10} is the reference wind speed 10 m above the water surface, U_{measured} is the measured wind speed at the height of the equipment (5 m above the water surface), z_0 is the water surface roughness length (set to 0.001 m) (Donelan et al. 1993; Johnson 1998), and z is the height of the meteorological station with reference to the water surface level.

Wind-wave- and current-induced shear stresses

The calculation of the shearing stress at the sediment–water interface, generated by wind-induced waves, is given by (Sheng and Lick 1979):

$$T_w = \rho f_w u_m^2 \cos\left(\frac{2\pi t}{T_s}\right) \cos\left(\frac{2\pi t}{T_s}\right), \quad (2)$$

where T_w is the wind-wave-induced shear stress, ρ is the water density, and f_w is the wave friction factor:

$$f_w = \exp\left[5.2\left(\frac{A_\delta}{Z_0}\right)^{-0.19} - 6.0\right], \quad (3)$$

where Z_0 is the roughness of the lake bottom taken as 0.2 mm (Nielsen et al. 2001; Qin et al. 2004), and A_δ is the wave-particle amplitude (m):

$$A_\delta = \frac{H_s}{2\sinh\left(\frac{2\pi h}{L_s}\right)}, \quad (4)$$

where u_m is the maximum orbital velocity of a wave near the bottom layer, t is the time variation, T_s is the significant wave period, and u_m can be expressed as (Madsen 1976):

$$u_m = \frac{\pi H_s}{T_s \sinh\left(\frac{2\pi h}{L_s}\right)}, \quad (5)$$

where L_s is the wavelength, h is the water depth, H_s is the significant wave height (m), and parameter L_s can be calculated as:

$$L_s = \left(\frac{gT_s^2}{2\pi}\right) \tanh\left(\frac{2\pi h}{L_s}\right). \quad (6)$$

The in situ shear stress produced by the bottom current was computed as follows (Sheng and Lick 1979; Hawley 2000):

$$T_c = \rho u_*^2, \quad (7)$$

where T_c (N/m^2) is the shear stress on the sediment surface, ρ ($10^3 \text{ kg}/\text{m}^3$) is the water density, and u_* (m/s) is the bottom shear velocity. The following equation was used to calculate u_* :

$$\frac{u_z}{u_*} = \frac{1}{\kappa} \ln\left(\frac{z}{z_0}\right), \quad (8)$$

where κ is von Karman's constant ($=0.4$), u_z is the flow velocity at height z above the sediment surface (in this study, $z=0.5 \text{ m}$), and z_0 is the value of the surface roughness ($=0.2 \text{ mm}$) (Nielsen et al. 2001; Qin et al. 2004).

Results

Wind speed and direction

The wind condition during the observation period was variable, and it could be divided into stable stages and transformation periods during the intervals between stable stages (Fig. 2). According to the wind direction and frequency statistics based on the data from site no. 1, no. 2, and no. 3, a northeast wind accounted for 74.9%, 67.8%, and 69.1% of the total measurements, respectively; thus, this was considered the prevailing wind direction during the observation period. Wind speed at site no. 1, no. 2, and no. 3 ranged from 0.25–9.82, 0.50–11.76, and 0.50–10.07 m/s, respectively, with average values of 4.37, 5.19, and 4.44 m/s, respectively. The distribution of wind speed conformed to a normal distribution, and the percentages of wind speeds in the range 3.00–8.00 m/s at site no. 1, no. 2, and no. 3 were 75.48%, 73.72%, and 70.09%, respectively. During the observation period, there were several steady and long-lasting periods of moderate wind (5.50–7.90 m/s; according to the Beaufort scale), which comprised a northeast wind from 11–17 September, 2–4 October, and 13–17 October, and a southeast wind from 29 September to 1 October. Before or after these periods, the wind condition was stable, and it took only 5 h for the transition from a southeast wind to a northeast wind on 11 October.

Wind waves

During 9 September to 17 October, the significant wave height and the wave period were observed in site no. 2 (Fig. 3). The significant wave height varied from 0.035 to 0.46 m with several peaks and intervals throughout the time series. The wind speed varied from 0.25 to 11.76 m/s and the wave period fluctuated around 2 s.

In association with the changing wind direction, wave height also changed considerably, as reflected in the large gaps between the peak wave heights during the time series (Fig. 3).

At 09:00 local time (LT) on 9 September 2017, the wind direction began to change from southeast to northwest. The wave height of 0.23 m dropped dramatically to 0.02 m over 7 h, before increasing to another maximum of 0.31 m 4 h later. During the period of wind direction change, the reduction of wave height was attributed to the decrease of wind speed, a process that can take 6–7 h. At 09:00 LT on 10 September 2017, the wind direction began to change from northwest to northeast, and eventually to east. However, the wind speed remained at about 6 m/s. During this period, the wave height of 0.41 m dropped dramatically to 0.21 m in 10 h. Later, when the wind speed dropped to around 4 m/s, the wave height declined further to 0.07 m over 5 h. This indicates that a change of wind direction can destroy the waves, whereas the wave height will be increased when the speed and direction of the wind remain reasonably constant. During the period from 17:00 LT on 13 September 2017 to 09:00 LT on 17 September 2017, the wind direction remained northeastward, with only minor changes, and the wind speed remained at around 6 m/s. Even though the wave height remained high, several drastic fluctuations were observed at the points of wind direction change.

Lake currents

Lake currents fluctuated considerably during the observation period. The temporal variations of current speeds and directions at different layers of the water column are illustrated in Fig. 4. According to the statistics, during the observation period, the average current speed in different layers ranged from 3.3 to 5.0 cm/s, and the current speed increased from the bottom layer to the surface layer. The slowest current was 0.1 cm/s and the fastest current was up to 39.0 cm/s.

Sediment resuspension during observation period

Turbidity fluctuated during the observation period (Fig. 5). There were several main peaks together with many minor

Fig. 2 Hourly wind velocity and direction at the three stations during the observation period

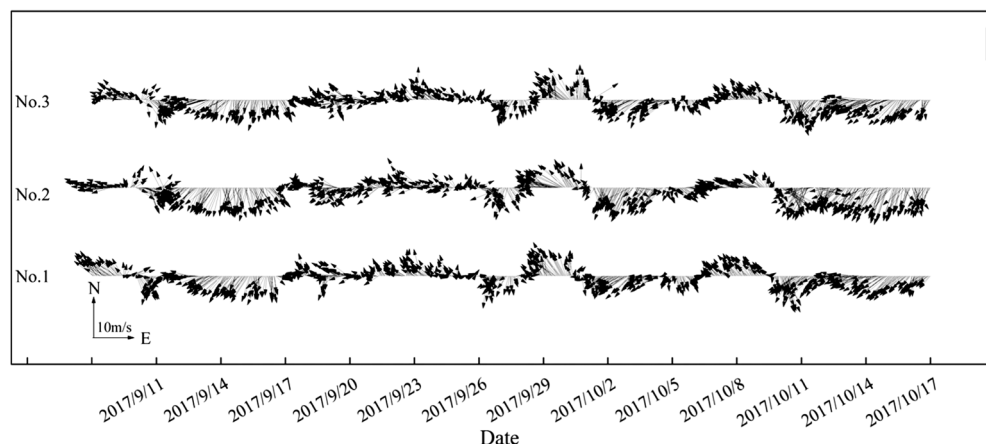
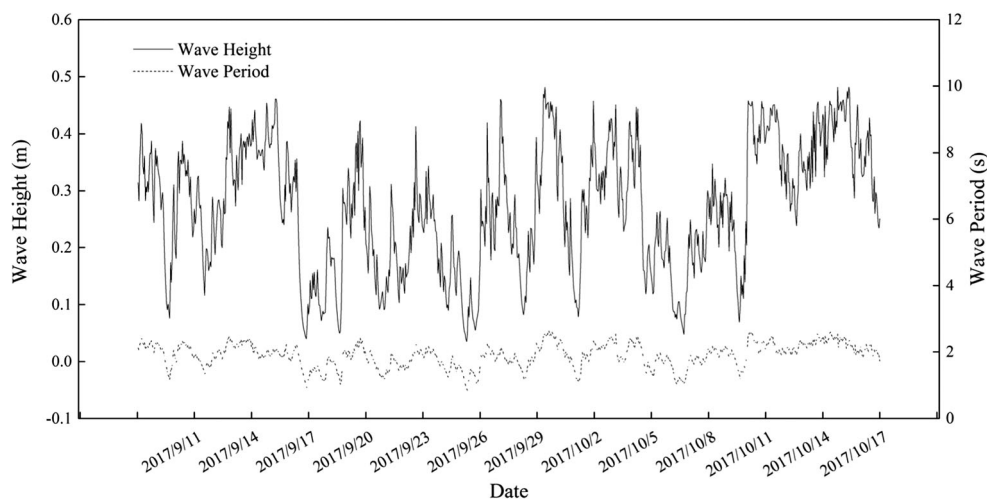


Fig. 3 Time series of hourly significant wave height and wave period



fluctuations during the principal changes. Measurements showed the turbidity of the water column varied from 36.4 to 158.7 NTU. Analysis of the turbidity data indicated that a background turbidity condition existed, and we set the lowest level of turbidity (36.5 NTU) as the maximum baseline turbidity. Among the peaks in turbidity, the maximum of 158.7 NTU was recorded at 10:00 LT on 17 September 2017, during a strong wind event with a wind speed of > 7 m/s. Generally, the turbidity peaks showed abrupt rises and falls; however, some turbidity events during periods of strong steady winds persisted for up to 76 h with turbidity of > 80.0 NTU, under long-lasting conditions of severe water disturbance.

Shear stresses of wind-induced waves and currents

The total shear stress comprised two components: wave-induced shear stress and current-induced shear stress. The former was much larger than the latter during the observation period, and the fluctuation of wave-induced shear stress was much greater than that of the current-induced shear stress

(Fig. 6). The shear stresses from wind-induced waves and currents were calculated using the equations in “Wind-wave-and current-induced shear stresses” section. Based on those calculations, the shear stress produced by waves ranged from 0.0437 to 0.338 N/m^2 , whereas the shear stress from currents varied from 0.002 to 0.127 N/m^2 . The combined total shear stress ranged from 0.0550 to 0.411 N/m^2 . The percentage of the total shear stress contributed by waves varied from 51.04 to 99.37%.

Discussion

The spatial heterogeneity of the wind field over water surface has been discussed in previous work (Ozger 2010; Vanem and Walker 2013). The wind data acquired in this study indicated that wind-induced waves and currents were influenced considerably by the wind condition and boundary reflection, especially during periods of low wind speed. This was revealed in the high level of synchronization between the wind speed,

Fig. 4 Lake currents in different layers. Layer 1, layer 2, layer 3, and layer 4 represent layers from the bottom of the water column to the surface part of the water column

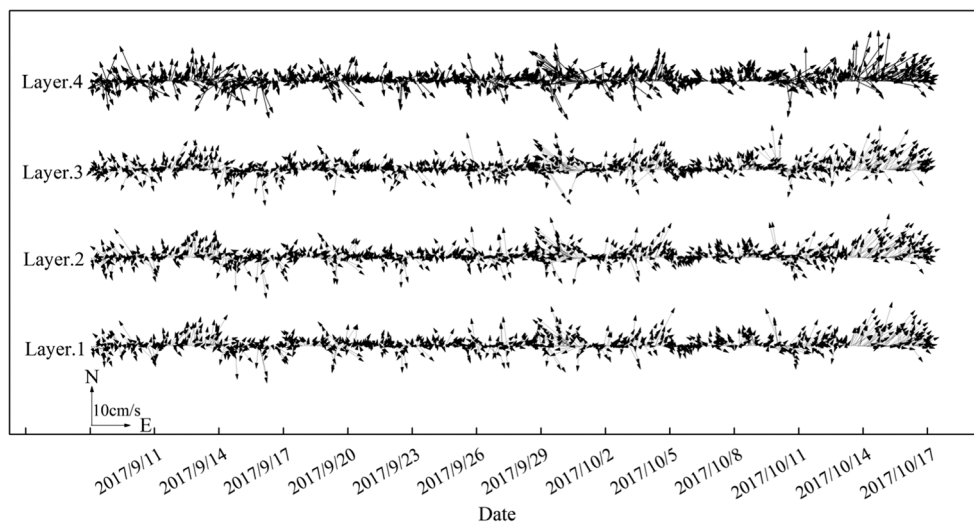
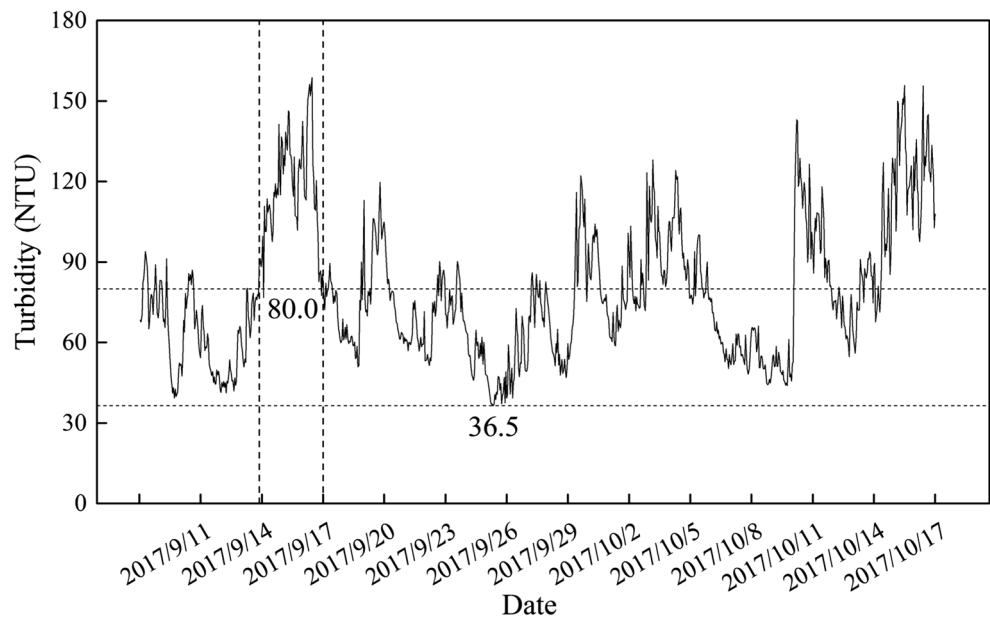


Fig. 5 Time series of hourly turbidity during the observation period



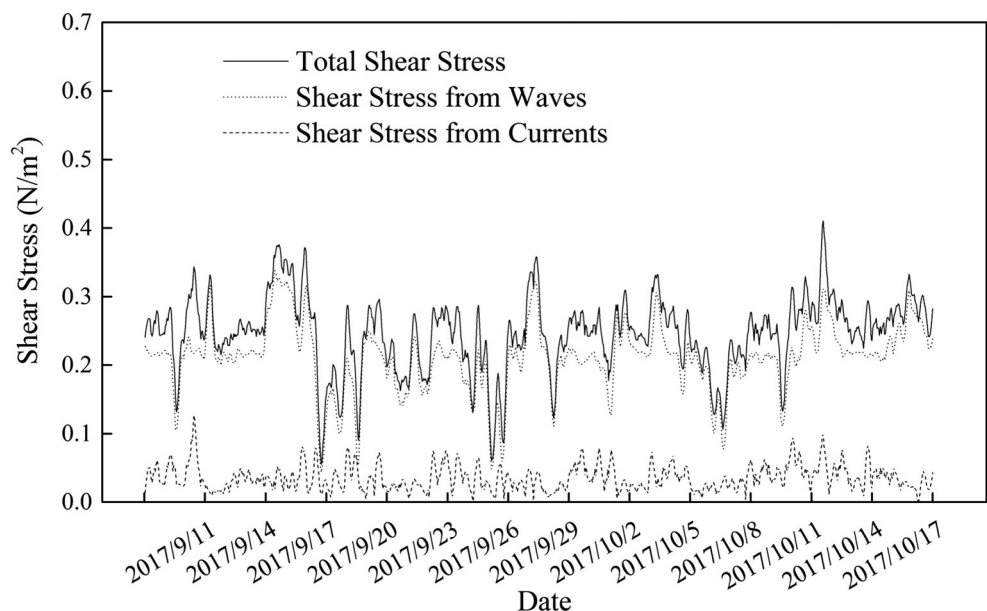
wave height, current speed, and shear stress. The following discussion introduces the relationship between wind, waves, and currents to explain their characteristics in Lake Taihu. Importantly, the relationships between wave- and current-induced shear stresses and sediment resuspension, during periods of increasing and decreasing turbidity, are discussed in detail to clarify the contributions of wave- and current-induced shear stresses to sediment resuspension during different hydrodynamic conditions.

Influence of wind on waves, currents, and turbidity

Many studies on the correlation between winds and waves (Cavaleri and Rizzoli 1981; Antenucci and Imberger 2003)

have lacked detailed discussion regarding the impact of different phases of wind speed. Based on analysis of the wind and wave time series data, we set the wind speed of 3.4 m/s as the boundary between light breeze (1.6–3.4 m/s) and gentle breeze (3.4–5.4 m/s) according to the Beaufort scale. The relationship between wind speed and wave height was found markedly different for high and low wind speeds based on the wind speed threshold of 3.4 m/s (Fig. 7a). For wind speeds < 3.4 m/s, wave height increased slowly as the wind speed increased. When the wind speed increased by 1.0 m/s, the wave height increased by 0.00852 m, on average. Conversely, for wind speeds > 3.4 m/s, wave height increased much more rapidly with increasing wind speed. As the wind speed increased

Fig. 6 Time series of shear stresses from waves and currents, and the total shear stress



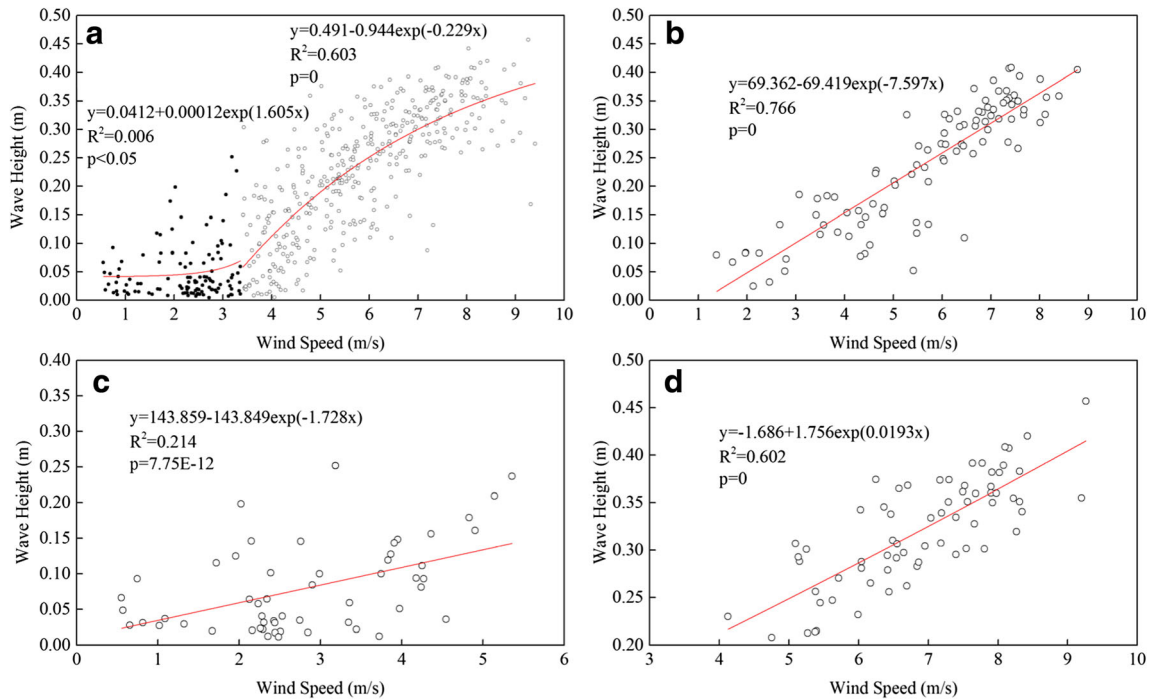


Fig. 7 **a** Plot of wave speed against wave height plot. The pattern comprises two components based on the threshold wind speed (3.4 m/s). **b** Correlation between wind speed and wave height during 9–12 September 2017 (an example of wind speed rising from low to high). **c**

Correlation between wind speed and wave height during 14–17 September 2017 (an example of low wind speed). **d** Correlation between wind speed and wave height during 17–20 September 2017 (an example of high wind speed)

by 1.0 m/s, the wave height increased by 0.0562 m, reflecting a growth rate 6.5 times that of the former case (wind speed < 3.4 m/s). In addition, the correlation of the

relationship between wind speed and wave height at low wind speeds ($R^2 = 0.006$) was weaker than for high wind speed ($R^2 = 0.603$).

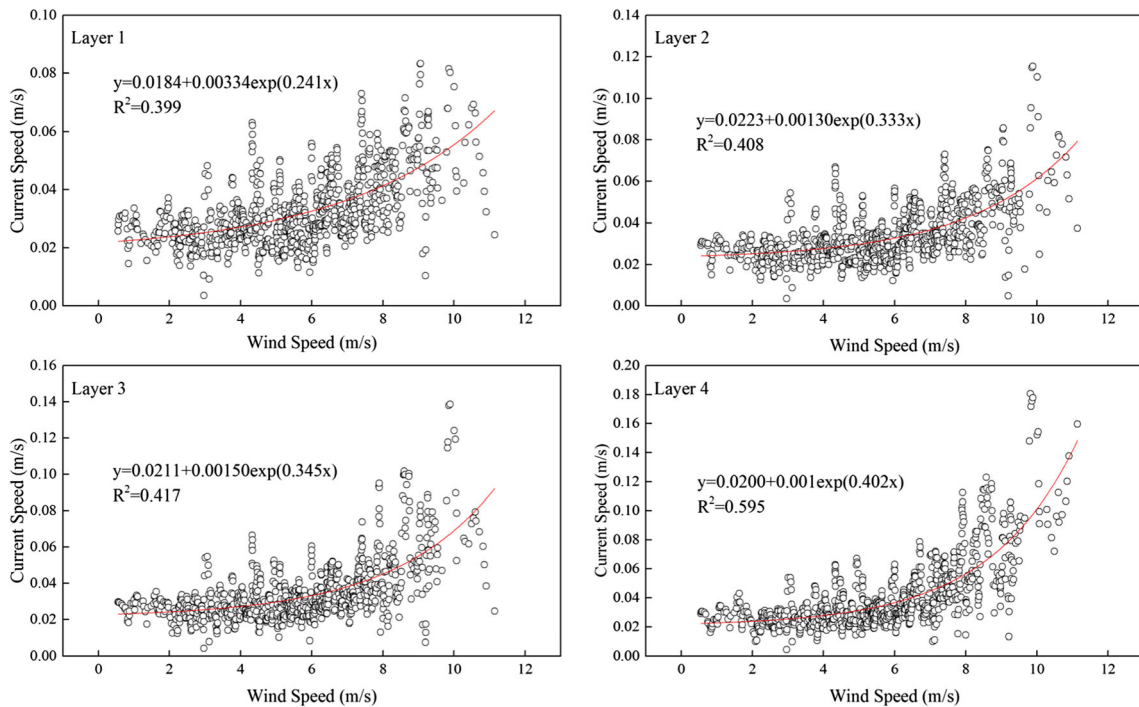
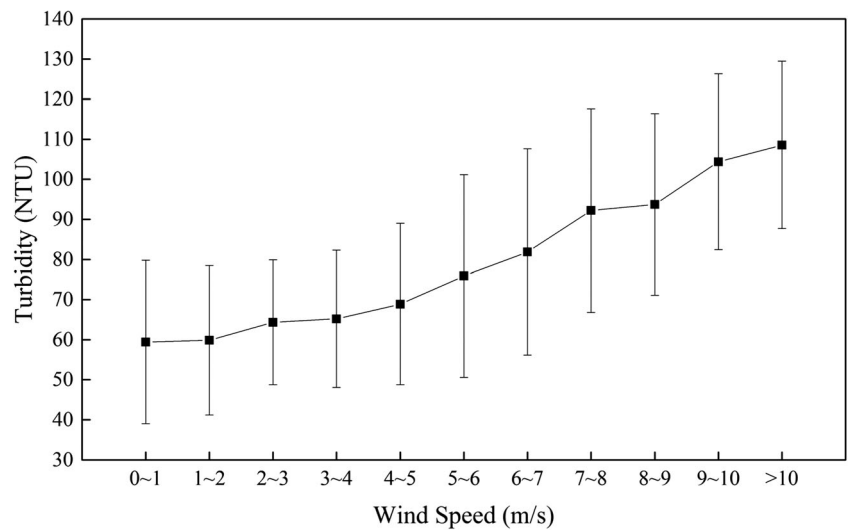


Fig. 8 Correlation between wind speed and current speed in different layers (layers from the bottom to the surface are layer 1, layer 2, layer 3, and layer 4)

Fig. 9 Plot of turbidity against wind speed, with error bars of turbidity for each stage of wind speed



We selected data from three different periods: 00:00 LT on 9 September to 22:00 LT on 12 September 2017 (high and low wind speeds), 18:00 LT on 24 September to 04:00 LT on 27 September 2017 (low wind speeds), and 12:00 LT on 14 September to 07:00 LT on 17 September 2017 (high wind speeds). For the first period, a strong relationship between wind speed and wave height was found ($R^2 = 0.766$). Among this series, the percentage of all samples with wind speed > 3.44 m/s was 88.42%. For the second period, the relationship between wind speed and wave height was found weak ($R^2 = 0.214$). The percentage of all samples with wind speed > 3.44 m/s was only 42.37%. For the third period, the relationship between wind speed and wave height was found strong ($R^2 = 0.602$). The percentage of all samples with wind speed > 3.44 m/s was 100%. The results indicated the relationship between wind speed and wave height was stronger during events with high wind speeds, and water depth was found a limiting factor for the growth of wave height.

It can be concluded that wave height will be changed by wind speed and wind direction, and that such change could possibly destroy the wave. If the wind condition becomes

constant and the wind speed becomes sufficiently strong, the wave height will be increased. However, increasing the wave height is difficult under conditions of low wind speed. This is because the stronger the wind is, the stronger the relationship will be between wind speed and wave height. This study proved that wave height is highly responsive to sudden changes in wind direction (Young et al. 2010).

Following studies in Lake Taihu, Wu et al. (2013) reported that the wind shear stress imposed on the water surface forces the surface water to move in the direction of the wind. A compensatory flow in the opposite direction was found in the bottom water; however, the middle layer water exhibited a complex movement state. The observational data and developed relationship between winds and currents in Qin et al. (2004) support this conclusion. However, the actual situation is much more complex. The results of this study showed that the directions of the currents in different layers, from the bottom to the surface, were similar, although the current speeds had some differences. Figure 8 shows the correlation between current speed and wind speed for the four layers from the bottom to the surface. The current of the layer closest to the surface had the strongest relationship with the wind. The R^2 values of the four layers from the surface to the bottom were 0.595, 0.417, 0.408, and 0.399, respectively. Therefore, when using wind condition to calculate sediment resuspension, the error associated with the current could be significant, while the effects from waves and currents will be confused.

The turbidity and wind data showed that turbidity generally increased with increasing wind speed with some uncertainties (Fig. 9) from 19.21 to 34.44%. The large fluctuation is because of the complex influence of wind on turbidity within the lake. Cózar et al. (2005) built mathematical formulas linking mean turbidity with wind speed.

Table 1 Series of starting and ending times of periods of sediment resuspension (takeoff) and deposition (landing)

Suspension stage	Starting time	Ending time	Duration (h)
Takeoff	2017.09.10 14:00	2017.09.11 11:00	22
	2017.09.14 09:00	2017.09.15 15:00	31
	2017.09.29 14:00	2017.09.30 07:00	17
Landing	2017.09.10 07:00	2017.09.10 13:00	7
	2017.09.17 09:00	2017.09.17 17:00	9
	2017.09.28 21:00	2017.09.29 04:00	8
	2017.10.06 18:00	2017.10.07 06:00	13

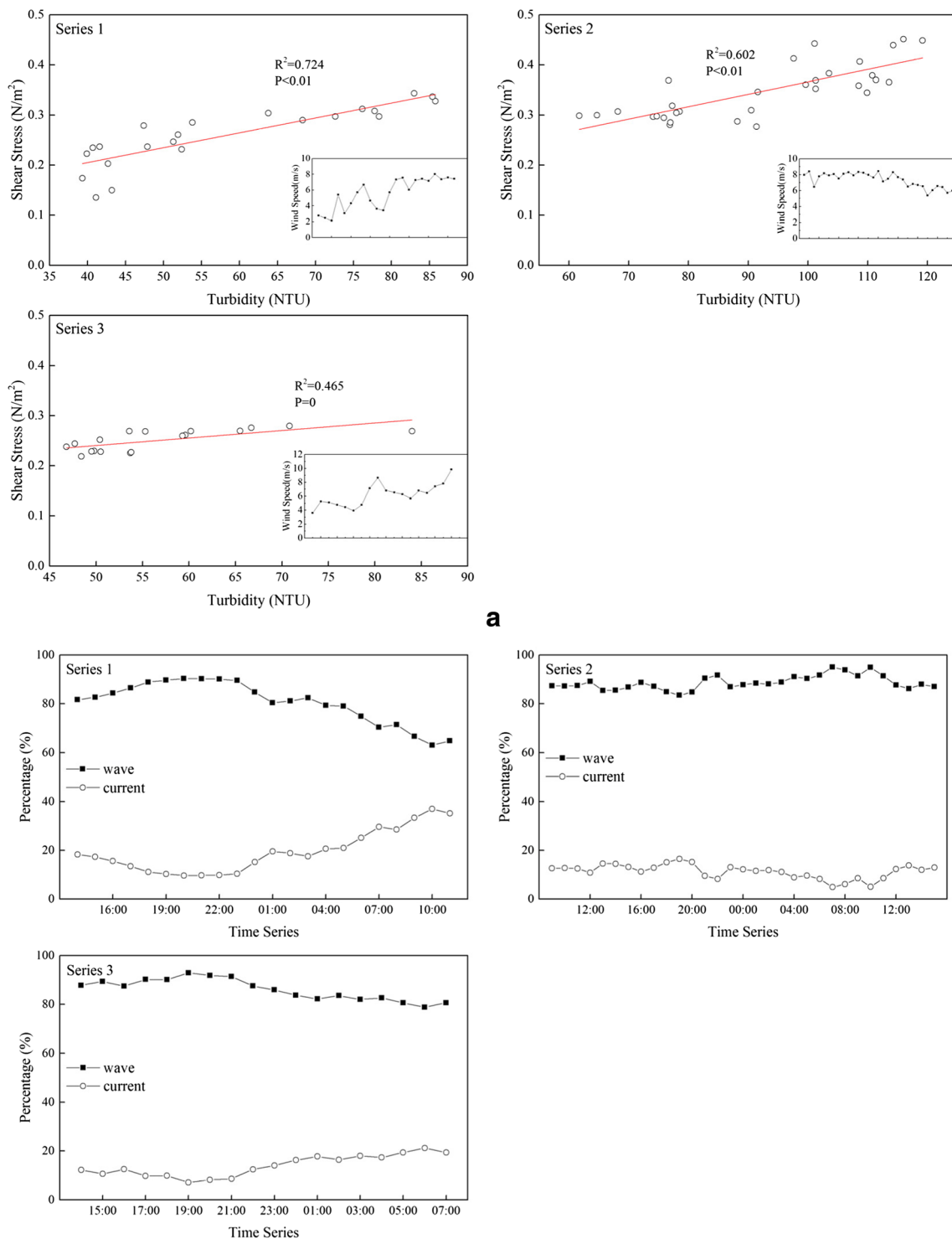


Fig. 10 **a** Correlation between shear stress and turbidity in three takeoff periods, together with the wind condition during these times. **b** Contributions of shear stress for sediment resuspension from wind-induced waves and currents during the period of rising shear stress

Driving forces of sediment resuspension

Water depth, macrophyte presence, wind fetch, and wind direction all have considerable impact on sediment resuspension (Hamilton and Mitchell 1996; Horppila and Nurminen 2001;

Gargett et al. 2004; James et al. 2004). However, previous studies on the relationship between wind speed and sediment resuspension have rarely quantified the hydrodynamic conditions, especially under different hydrodynamic phases (Booth et al. 2000; Shinohara and Isobe 2010; Zheng et al. 2015),

which constitute one of the most important factors for sediment resuspension. The physical processes within the water column directly affect sediment resuspension. The relationship between wind-induced waves and turbidity, and the relationship between current and turbidity are both more important than that between wind and sediment resuspension, especially in the development of hydrodynamic models. In addition, the shear stresses produced by wind-induced waves and currents are more easily quantified, making it easier to determine whether sediment resuspension will occur and how much sediment might be brought into the water column. Furthermore, the hydrodynamic impact on bottom sediment is the key to understanding the mechanism of sediment resuspension, and the release of nitrogen from the sediment.

In this study, we calculated the bottom shear stresses from wind-induced waves and currents, and we quantified their contributions to provide a more reasonable method for the simulation of sediment resuspension in shallow lakes such as Lake Taihu. The series selected in this case was divided into two groups: the first group was the period of increasing shear stress, and the second group was the period of declining shear stress. The details of the series are shown in Table 1.

For the period of increasing shear stress, the linear relationship between turbidity and shear stress is shown in Fig. 10a. Regression analysis revealed that the R^2 values between the shear stress and turbidity of the three datasets shown in Fig. 10a were 0.724, 0.602, and 0.465 (Table 2). The wind speed in series 1 and 3 increased with time (i.e., from 2.12 and 3.63 m/s to 8.01 and 9.83 m/s, respectively), whereas the wind speed in series 2 remained high (i.e., > 6 m/s). The contributions of shear stress from wind-induced waves dropped from 81.69 to 64.82% in series 1 and from 89.42 to 78.84% in series 3. The percentages of shear stress from currents increased from 18.31 to 35.18% in series 1 and from 10.58% to 21.16% in series 3. The contribution of waves to shear stress in series 2 was also > 80%.

Table 2 Correlation between shear stress and turbidity, and contributions of different shear stresses to turbidity (R^2 -1, correlation coefficients between total shear stress and turbidity; R^2 -2, correlation coefficients between wave-induced shear stress and turbidity; R^2 -3, correlation coefficients between current-induced shear stress and turbidity; WT-1, contribution from wave-induced shear stress; WT-2, contribution from current-induced shear stress)

Suspension stage		R^2 -1	R^2 -2	R^2 -3	WT-1	WT-2
SPM takeoff	Series 1	0.72	0.24	0.84	80.58	19.42
	Series 2	0.60	0.71	-0.03	88.69	11.31
	Series 3	0.47	0.13	0.60	86.07	13.93
SPM landing	Series 4	0.92	0.91	0.61	75.09	24.91
	Series 5	0.70	0.79	0.45	71.39	28.61
	Series 6	0.99	0.98	0.25	94.14	5.86
	Series 7	0.82	0.74	-0.04	86.42	13.58

These findings indicate that during the initial period of development of waves and currents, the impacts of waves and currents on sediment resuspension were markedly different. As waves are sensitive to influence from the wind, the waves developed quickly and caused sediment resuspension. However, the currents responded slowly to the wind and they had very limited impact on sediment resuspension. Difference was also evident in the percentages of the shear stresses contributed by waves and currents to sediment resuspension. Along with the development of the waves and currents, the contribution of current-induced shear stress to sediment resuspension gradually increased.

When the development of waves and currents reach certain degrees, such as when the drag force from the wind on the surface of the water column is balanced by the friction at the bottom of the water column, the development of the current will cease and an equilibrium state will be formed. Thus, the contributions of shear stresses from waves and currents will become relatively stable. In series 2, the contribution of shear stress from waves accounted for the largest percentage, which remained around 90% with minimal fluctuation. In these three series, the combined shear stresses all increased with time because of the energy input from the wind. This shows that, at the initial period of sediment resuspension, the driving force was predominantly wave-induced shear stress, which was the “pioneer” shear stress for sediment resuspension. However, the current-induced shear stress gradually increased as another driving force for sediment resuspension.

In the period of declining shear stress, the wind speed dropped from approximately 6 to 1 m/s (Fig. 11). The shear stress and turbidity showed strong correlation with R^2 values of 0.915, 0.702, 0.987, and 0.823. In these periods, the input energy reduced with the decreasing wind speed. Because waves are more sensitive than currents to the wind, the decrease of wind speed resulted in weakening of the waves. However, the currents were relatively unaffected by the decrease of wind speed. The percentage of wave-induced shear stress for sediment resuspension decreased with wind speed more quickly than that of the currents. The percentages of wave-induced shear stress had minor declines in these four series, while the percentages of current-induced shear stress remained greater. However, in series 4, 5, and 7, the percentages of wave-induced shear stress rose again, which indicated that the current speed had been influenced by the decrease of wind speed during these hours, which meant that the percentages of the current-induced shear stress decreased.

Conclusions

This study found that the wind in Lake Taihu had spatial heterogeneity, especially when the wind speed was low.

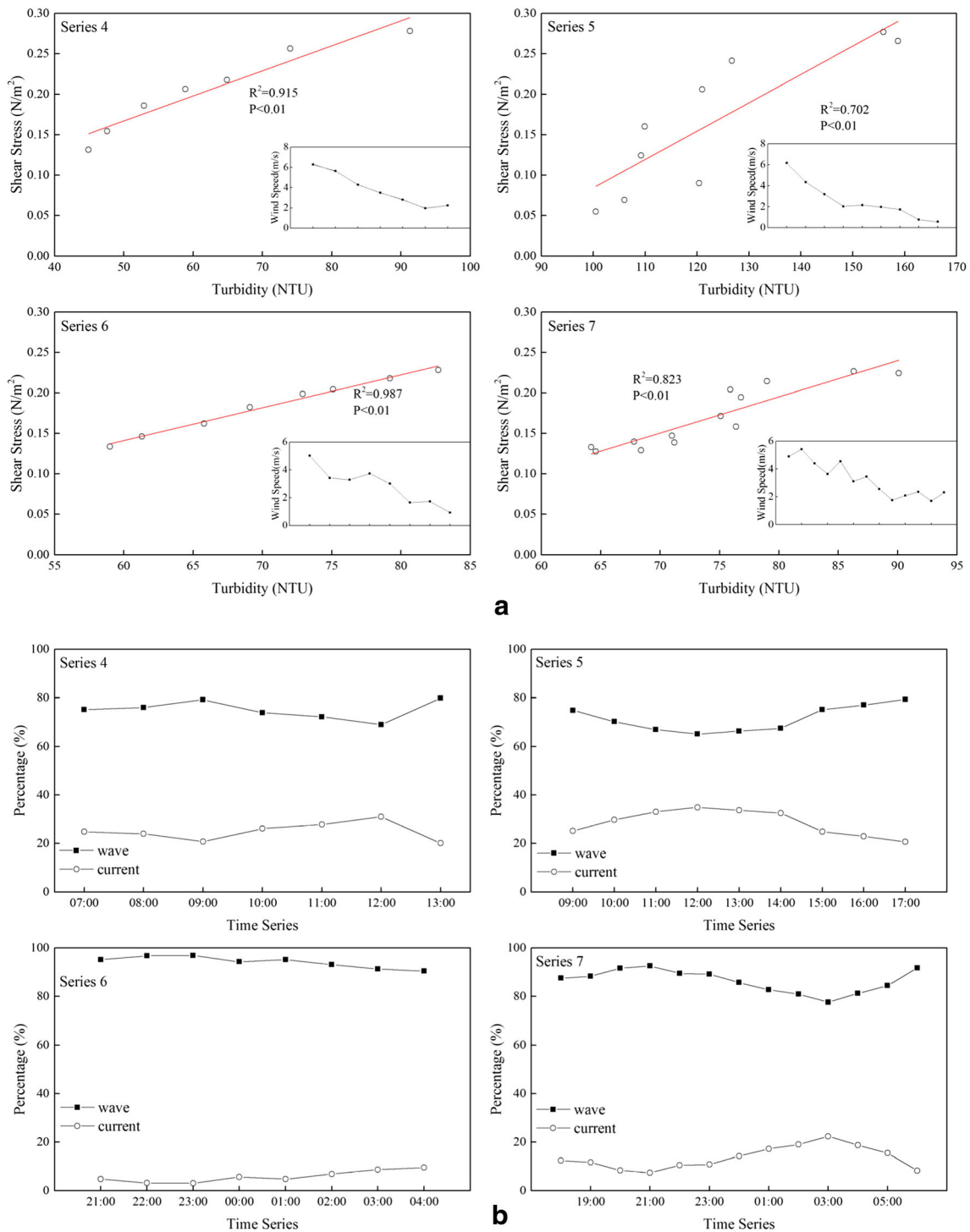


Fig. 11 **a** Correlation between shear stress and turbidity in the four landing periods, together with the wind condition during these times. **b** Contributions of the shear stress for sediment resuspension between wind-induced waves and currents during the period of declining shear stress

With an increase of wind speed, this heterogeneity decreased, and the wind became the dominant factor influencing the currents, waves, and turbidity. The current speed in Lake Taihu ranged from 0.06 to 36.75 cm/s, and the average speed of all the samples varied from 3.3 to 5.0 cm/s from the bottom to the surface. We obtained an equation for the relationship between

wave height and wind speed: $wave\ height = 0.491 - 0.944e^{-0.229wind\ speed}$. It is acknowledged that wave height will be limited by the depth of the lake, and the highest wave will be approximately 0.45 m.

The physical processes within the water column had direct impact on sediment resuspension. In the different stages of

sediment resuspension, the relative contributions from waves and currents could be changed because of their different responses to the wind. In the period of rising shear stress, the percentage of shear stress from waves began at a high level (> 85%) but dropped with the development of the current. However, during the period of decreasing shear stress, the percentage of shear stress from waves initially dropped before increasing with the decrease of current speed.

Acknowledgments We are grateful for grants and support from the National Key R&D Program of China (2017YFC0405205), National Natural Science Foundation of China (No. 41621002), Major Projects on Control and Rectification of Water Body Pollution (2017ZX07203), International Scientific Cooperation Project (4161101120), and Key Research Program of Frontier Sciences of the Chinese Academy of Sciences (QYZDJSSWDQC008).

References

- Amos CL, Mosher DC (1985) Erosion and deposition of fine-grained sediments from the Bay of Fundy. *Sedimentology* 32:815–832
- Antenucci JP, Imberger J (2003) The seasonal evolution of wind/internal wave resonance in Lake Kinneret. *Limnol Oceanogr* 48:2055–2061
- Bailey MC, Hamilton DP (1997) Wind induced sediment resuspension: a lake-wide model. *Ecol Model* 99:217–228
- Booth JG, Miller RL, McKee BA, Leathers RA (2000) Wind-induced bottom sediment resuspension in a microtidal coastal environment. *Cont Shelf Res* 20:785–806
- Cavaleri L, Rizzoli PM (1981) Wind wave prediction in shallow water: theory and applications. *J Geophys Res* 86:10961–10973
- CERC (1984) Shore protection manual V.1. U.S Army Coastal Eng. Res Center, Ft Belvoir
- Chen Y, Chen S, Liu J, Yao M, Sun W, Zhang Q (2013) Environmental evolution and hydrodynamic process of Dongping Lake in Shandong Province, China, over the past 150 years. *Environ Earth Sci* 68:69–75
- Chung EG, Bombardelli FA, Schladow SG (2009) Sediment resuspension in a shallow lake. *Water Resour Res* 45:5422
- Cózar A, Gálvez JA, Hull V, García CM, Loiselle SA (2005) Sediment resuspension by wind in a shallow lake of Esteros del Iberá, (Argentina): a model based on turbidimetry. *Ecol Model* 186:63–76
- Donelan MA, Dobson FW, Smith SD, Anderson RJ (1993) On the dependence of sea surface roughness on wave development. *J Phys Oceanogr* 23:2143–2149
- Gargett A, Wells J, Tejada-Martínez AE, Grosch CE (2004) Langmuir supercells: a mechanism for sediment resuspension and transport in shallow seas. *Science* 306:1925–1928
- Hamilton DP, Mitchell SF (1996) An empirical model for sediment resuspension in shallow lakes. *Hydrobiologia* 317:209–220
- Hawley N (2000) Sediment resuspension near the Keweenaw Peninsula, Lake Superior during the fall and winter 1990–1991. *J Great Lakes Res* 26:495–505
- Horpila J, Nurminen L (2001) The effect of an emergent macrophyte (*Typha angustifolia*) on sediment resuspension in a shallow north temperate lake. *Freshw Biol* 46:1447–1455
- Huang J, Xu Q, Xi B, Wang X, Li W, Gao G, Huo S, Xia X, Jiang T, Ji D, Liu H, Jia K (2015) Impacts of hydrodynamic disturbance on sediment resuspension, phosphorus and phosphatase release, and cyanobacterial growth in Lake Tai. *Environ Earth Sci* 74:3945–3954
- Hu C, Hu W, Zhang F, Hu Z, Li X, Chen Y (2006) Sediment resuspension in the Lake Taihu, China. *Chin Sci Bull* 51:731–737
- James RT, Martin J, Wool T, Wang PF (1997) A sediment resuspension and water quality model of lake okeechobee. *J Am Water Resour Assoc* 33:661–678
- James WF, Barko JW, Butler MG (2004) Shear stress and sediment resuspension in relation to submersed macrophyte biomass. *Hydrobiologia* 515:181–191
- Jin KR, Sun D (2007) Sediment resuspension and hydrodynamics in Lake Okeechobee during the late summer. *J Eng Mech* 133:899–910
- Ji Z, Jin K (2014) Impacts of wind waves on sediment transport in a large, shallow lake. *Lakes Reserv Res Manag* 19:118–129
- Johnson HK (1998) On the dependence of sea surface roughness on wind waves. *J Phys Oceanogr* 28:1702–1716
- Koch EW (1999) Sediment resuspension in a shallow *Thalassia testudinum*, banks ex König bed. *Aquat Bot* 65:269–280
- Lawson SE (2004) Sediment suspension as a control on light availability in a coastal lagoon. Dissertation, Univ. of Va
- Lawson SE, Mcglathery KJ, Wiberg PL (2012) Enhancement of sediment suspension and nutrient flux by benthic macrophytes at low biomass. *Mar Ecol Prog Ser* 448:259–270
- Li D, Huang Y, Fan C, Yuan Y (2011) Contributions of phosphorus on sedimentary phosphorus bioavailability under sediment resuspension conditions. *Chem Eng J* 168:1049–1054
- Luettich RA, Somlyódy L (1990) Dynamic behavior of suspended sediment concentrations in a shallow lake perturbed by episodic wind events. *Limnol Oceanogr* 35:1050–1067
- Madsen OS (1976) Wave climate of the continental margin: elements of its mathematical description. In: Stanley DJ, Swift DJP (eds) *Marine sediment transport and environmental management*. John Wiley & Sons, New York, p 65–87
- Ma JR, Qin BQ, Hans WP, Justin DB, Nathan SH, Shi K, Zhou YQ, Guo JS, Li Z, Xu H, Wu TF, Long SX (2016) The persistence of cyanobacterial (*Microcystis* spp.) blooms throughout winter in Lake Taihu, China. *Limnol Oceanogr* 61(2):711–722
- Ma JR, Justin DB, Qin BQ, Hans WP, Gao G, Wu P, Zhang W, Deng JM, Zhu GW, Zhang YL, Xu H, Niu HL (2014) Environmental factors controlling colony formation in blooms of the cyanobacteria *Microcystis* spp. in Lake Taihu, China. *Harmful Algae* 31:136–142
- Mehta AJ, Hwang KN, Khare YP (2015) Critical shear stress for mass erosion of organic-rich fine sediments. *Estuar Coast Shelf Sci* 165:97–103
- Møller LF, Riisgård HU (2007) Impact of jellyfish and mussels on algal blooms caused by seasonal oxygen depletion and nutrient release from the sediment in a Danish fjord. *J Exp Mar Biol Ecol* 351:92–105
- Nielsen P, Robert S, Møller-Christiansen B, Oliva P (2001) Infiltration effects on sediment mobility under waves. *Coast Eng* 42:105–114
- Olsson S, Regnéll J, Persson A, Sandgren P (1997) Sediment-chemistry response to land-use change and pollutant loading in a hypertrophic lake, southern Sweden. *J Paleolimnol* 17:275–294
- Ozger M (2010) Significant wave height forecasting using wavelet fuzzy logic approach. *Ocean Eng* 37:1443–1451
- Paul JF, Kasprzyk R, Lick W (1982) Turbidity in the Western Basin of Lake Erie. *J Geophys Res* 87:5779–5784
- Preusse M, Peeters F, Lorke A (2010) Internal waves and the generation of turbulence in the thermocline of a large lake. *Limnol Oceanogr* 55:2353–2365
- Qin BQ (2008) *Lake Taihu, China*. Springer, New York
- Qin B, Hu W, Gao G (2004) Dynamics of sediment resuspension and the conceptual schema of nutrient release in the large shallow Lake Taihu, China. *Sci Bull* 49:54–64
- Qin B, Zhu G, Gao G, Zhang Y, Li W, Paerl HW, Carmichael WW (2010) A drinking water crisis in Lake Taihu, China: linkage to climatic variability and lake management. *Environ Manag* 45:105–112
- Qin B, Zhu G, Zhang L, Luo L, Gao G, Gu BH (2006) Estimation of internal nutrient release in large shallow Lake Taihu, China. *Sci China Ser D Earth Sci* 49:38–50

- Qin B, Xu P, Wu Q, Luo L, Zhang Y (2007) Environmental issues of Lake Taihu, China. *Hydrobiologia* 581:3–14
- Sheng YP, Lick W (1979) The transport and resuspension of sediments in a shallow lake. *J Geophys Res* 84:1809–1826
- Shinohara R, Isobe M (2010) Daily change in wind-induced sediment resuspension and phosphorus forms in a shallow eutrophic lake. *Fundam Appl Limnol* 176:161–171
- Søndergaard M, Kristensen P, Jeppesen E (1992) Phosphorus release from resuspended sediment in the shallow and wind-exposed Lake Arresø, Denmark. *Hydrobiologia* 228:91–99
- Stastna M, Lamb KG (2008) Sediment resuspension mechanisms associated with internal waves in coastal waters. *J Geophys Res* 113:1–19
- Tan X (2012) Physiological and ecological characteristics in the life cycle of bloom-forming cyanobacteria. *J Food Agric Environ* 10:929–934
- Vanem E, Walker SE (2013) Time series analysis of significant wave height data for identification of trends in the ocean wave climate. *International Conference on Ocean, Offshore and Arctic Engineering* 148–160
- Wang J, Pang Y, Li Y, Huang Y, Luo J (2015) Experimental study of wind-induced sediment suspension and nutrient release in Meiliang Bay of Lake Taihu, China. *Environ Sci Pollut Res* 22:10471–10479
- Wiberg PL (2007) Wind-driven sediment suspension controls light availability in a shallow coastal lagoon. *Estuar Coasts* 30:102–112
- Wilcock PR (1993) Critical shear stress of natural sediments. *J Hydraul Eng* 119:491–505
- Wu T, Qin B, Zhu G, Luo L, Ding Y, Bian G (2013) Dynamics of cyanobacterial bloom formation during short-term hydrodynamic fluctuation in a large shallow, eutrophic, and wind-exposed Lake Taihu, China. *Environ Sci Pollut Res* 20:8546–8556
- Yan D, Wünnemann B, Hu Y, Frenzel P, Zhang Y, Chen K (2017) Wetland evolution in the Qinghai Lake area, China, in response to hydrodynamic and eolian processes during the past 1100 years. *Quat Sci Rev* 162:42–59
- Young IR, Hasselmann S, Hasselmann K (2010) Computations of the response of a wave spectrum to a sudden change in wind direction. *J Phys Oceanogr* 17:1317–1338
- Zhao Q, Wang J, Wang J, Wang JXL (2018) Seasonal dependency of controlling factors on the phytoplankton production in Taihu Lake, China. *J Environ Sci*. <https://doi.org/10.1016/j.jes.2018.05.010>
- Zheng SS, Wang PF, Wang C, Hou J (2015) Sediment resuspension under action of wind in Taihu Lake China. *Int J Sediment Res* 30:48–62
- Zhu L, Li X, Zhang C, Duan Z (2017) Pollutants' release, redistribution and remediation of black Smelly River sediment based on resuspension and deep aeration of sediment. *Int J Environ Res Public Health* 14:374